DOI: 10.1002/ejic.201000057

Ferromagnetic Tetranuclear and Pentanuclear Copper(II) Complexes Constructed from Cu_2 Blocks

Matilde Fondo,*[a] Noelia Ocampo,[a] Ana M. García-Deibe,[a] and Jesús Sanmartín[b]

Keywords: Carboxylate ligands / Copper / Cluster compounds / Magnetic properties / Schiff bases

The new complexes $[(Cu_2L^1)_2(p\text{-}OOC\text{-}C_6H_4\text{-}COO)]\cdot 7H_2O$ (**1**·$7H_2O$), $[(Cu_2L^2)_2(p\text{-}OOC\text{-}C_6H_4\text{-}COO)]\cdot 2H_2O$ (**2**·$2H_2O$), $[(Cu_2L^1)_2Cu(O_2C\text{-}CH_2\text{-}CO_2)_2]\cdot 9H_2O$ (**3**·$9H_2O$) and $[(Cu_2L^2)_2(OOC\text{-}CH_2\text{-}COO)]\cdot 5.5H_2O$ (**4**·$5.5H_2O$) have been obtained by interaction of either $[(Cu_2L^1)_2(CO_3)]\cdot 8H_2O$ or $[Cu_2L^2(OH)]\cdot 1.125H_2O$ with the corresponding dicarboxylic acid. Recrystallisation of **1**·$7H_2O$ in methanol/ethanol yields single crystals of **1**·2EtOH·$2H_2O$, whereas recrystallisation of **3**·$9H_2O$ and **4**·$5.5H_2O$ in methanol allows crystals of **3**·$9H_2O$ and **4**·$5.5H_2O$·1.25MeOH, respectively, to be isolated, which were suitable for X-ray diffraction studies. The X-ray characterisation of **1**·2EtOH·$2H_2O$, **3**·$9H_2O$ and **4**·$5.5H_2O$·1.25MeOH shows that both the Cu_4 and Cu_5 clusters can be understood as being built from two dinuclear $[Cu_2L^x]^+$ (x = 1 or 2) blocks with different connectors. Magnetic analyses of **1**·$7H_2O$, **3**·$9H_2O$ and **4**·$5.5H_2O$ reveal that the three complexes are ferromagnetic, and the magnetic exchange mediated by the carboxylate ligands is weak.

Introduction

The synthesis and characterisation of polynuclear 3d metal complexes has attracted intense study, because they are of prime importance in the area of molecular magnetism.[1–4] Thus, the chance of discovering new molecular magnets will profit from the continuous development of synthetic procedures for polynuclear species. Actually, various methods have been worked out, but the final outcome can be rarely predicted beforehand. In this way, the node and spacer approach[5] is maybe one of the most foreseeable synthetic methods, where the topology of the compound and even its nuclearity can be modulated by choosing the appropriate metal ion and bridging ligand.

We have reported that a certain kind of compartmental Schiff base ligand (Scheme 1) can easily yield dinuclear complexes of the type $[M_2LL']$.[6] This kind of complex always shows an exogenous bridge (L′) that can be simply replaced. In addition, the magnetic interaction between the two metal ions allocated in the ligand pockets is always ferromagnetic in nature, an unusual feature promoted by the presence of a NCN imizadolidine bridge, as it could be demonstrated by DFT calculations.[7] Thus, it seems that the $[M_2L]^+$ fragments can be exploited as tectons of predefined ground state. Consequently, the use of suitable crosslinking ligands between these dinuclear units could be a route to produce complexes of higher nuclearity, with a total spin sum of the individual spins of the initial nodes.

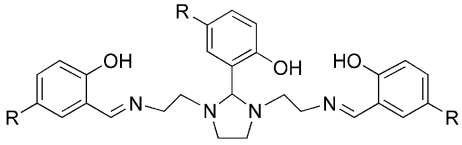

Scheme 1.

Among bridging ligands, dicarboxylates have been widely studied and their magnetic behaviour has been mainly analysed in copper complexes.[8–10] From these studies, it becomes apparent that some coordination modes of terephthalate and malonate donors mediate a ferromagnetic coupling. With these considerations in mind, we decided to investigate the structure and magnetic behaviour of copper complexes constructed from $[Cu_2L]^+$ blocks, bridged by terephthalate or malonate ligands. The results achieved are reported herein.

Results and Discussion

Interaction of the related microcrystalline products $[(Cu_2L^1)_2(CO_3)]\cdot 8H_2O$[7a] or $[Cu_2L^2(OH)]\cdot 1.125H_2O$[6c] ($H_3L^1$ and H_3L^2 in Scheme 1) with terephthalic acid leads to tetranuclear complexes of the type $[(Cu_2L^x)_2(p\text{-}OOC\text{-}C_6H_4\text{-}COO)]\cdot nH_2O$ [x = 1, n = 7 (**1**·$7H_2O$) or x = 2, n = 2

[a] Departamento de Química Inorgánica, Facultade de Ciencias, Universidade de Santiago de Compostela, 27002 Lugo, Spain
E-mail: matilde.fondo@usc.es
[b] Departamento de Química Inorgánica, Facultade de Química, Universidade de Santiago de Compostela, 15782 Santiago de Compostela, Spain

Supporting information for this article is available on the WWW under http://dx.doi.org/10.1002/ejic.201000057.

($2{\cdot}2H_2O$)], showing the displacement of the carbonate or hydroxide exogenous ligands by the terephthalate one. However, when a similar reaction is performed with the use of malonic acid instead of terephthalic acid, the nuclearity of the obtained complex seems to depend on the nature of the Schiff base donor. Thus, with $[L^1]^{3-}$ the pentanuclear cluster $[(Cu_2L^1)_2Cu(O_2C\text{-}CH_2\text{-}CO_2)_2]{\cdot}9H_2O$ ($3{\cdot}9H_2O$) is obtained, whereas the presence of $[L^2]^{3-}$ leads to the tetranuclear complex $[(Cu_2L^2)_2(OOC\text{-}CH_2\text{-}COO)]{\cdot}5.5H_2O$ ($4{\cdot}5.5H_2O$). Regardless of this, the performed experiments clearly show that the tested synthetic method constitutes a route to isolate complexes of higher nuclearity that are based on dinuclear $[Cu_2L^x]^+$ (x = 1, 2) blocks.

Complexes $1{\cdot}7H_2O$ to $4{\cdot}5.5H_2O$ were fully characterised by analytical, spectroscopic and spectrometric methods. Besides, recrystallisation of microcrystalline samples of $1{\cdot}7H_2O$ in methanol/ethanol and that of $3{\cdot}9H_2O$ and $4{\cdot}5.5H_2O$ in methanol yields single crystals of $1{\cdot}2EtOH{\cdot}2H_2O$, $3{\cdot}9H_2O$ and $4{\cdot}5.5H_2O{\cdot}1.25MeOH$, respectively, suitable for X-ray diffraction studies. Accordingly, $1{\cdot}2EtOH{\cdot}2H_2O$, $3{\cdot}9H_2O$ and $4{\cdot}5.5H_2O{\cdot}1.25MeOH$ could be also crystallographically characterised. In addition, complexes $1{\cdot}7H_2O$, $3{\cdot}9H_2O$ and $4{\cdot}5.5H_2O$ were additionally analysed by magnetic studies.

The infrared spectra of all the compounds contain a sharp band at ca. 1630 cm^{-1}, in agreement with the coordination of the Schiff base to the metal ions through the imine nitrogen atoms. Besides, it should be noted that the high number of bands about 1600 cm^{-1} (due to C=C, C–$O_{phenolic}$, and C=N bonds) prevents the unambiguous assignment of the C–O stretching modes of the carboxylate ligands.[11] In addition, the ESI mass spectra of all the complexes show a main peak with mass and isotopic distribution patterns related to the fragments $[Cu_2L^x]^+$ (x = 1, 2). No peaks related to the whole molecules could be detected, maybe owing to their neutral character.

Description of the Crystal Structure

Single crystals of $1{\cdot}2EtOH{\cdot}2H_2O$, $3{\cdot}9H_2O$ and $4{\cdot}5.5H_2O{\cdot}1.25MeOH$, suitable for X-ray diffraction studies, were grown as detailed in the Experimental Section.

1·2EtOH·2H₂O

An ORTEP view of **1** is shown in Figure 1. Main distances and angles are listed in Table 1, and experimental details are given in Table 5.

Table 1. Main bond lengths (Å) and angles (°) for $1{\cdot}2EtOH{\cdot}2H_2O$.[a]

Cu11–O101	1.9339(12)	Cu12–O102	1.9126(11)
Cu11–N101	1.9446(13)	Cu12–O103	1.9425(10)
Cu11–O10	1.9495(11)	Cu12–N102	1.9448(13)
Cu11–N103	2.1101(13)	Cu12–N104	2.0580(13)
Cu11–O103	2.2762(11)		
Cu11···Cu12	3.2454(3)	Cu11···Cu12′	10.2545(4)
N101–Cu11–O10	173.83(5)	O103–Cu12–N102	155.97(5)
O101–Cu11–N103	171.92(5)	O102–Cu12–N104	172.83(5)
Cu11–O103–Cu12	100.28(5)		

[a] Symmetry operation ′ = –x, –y, –z.

The crystal structure of $1{\cdot}2EtOH{\cdot}2H_2O$ shows that it is a tetranuclear complex, with ethanol and water molecules as solvates. The neutral complex $[(Cu_2L^1)_2(p\text{-}OOC\text{-}C_6H_4\text{-}COO)]$ can be considered as self-assembled from two dinuclear $[Cu_2L^1]^+$ nodes joined by a doubly deprotonated terephthalate ligand. The compound shows an inversion centre located on the centroid of the aromatic ring of the dicarboxylate donor and, accordingly, both $[Cu_2L^1]^+$ cations are crystallographically equivalent.

In each dinuclear unit, the Schiff base acts as an heptadentate dicompartmental donor, allocating a copper ion in each one of its N_2O compartments (N_{amine}, N_{imine}, O_{phenol}). In addition, the central phenol oxygen atom O103 bridges the two metal atoms of the same dinuclear cation.

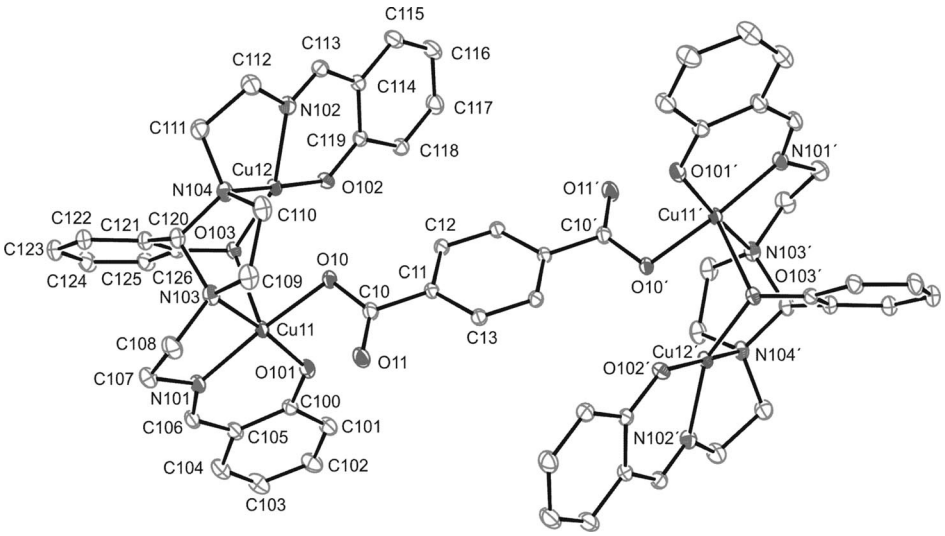

Figure 1. An ORTEP view of the crystal structure of **1**. Hydrogen atoms are omitted for clarity. Ellipsoids are drawn at 40% probability.

Both $[Cu_2L^1]^+$ nodes are joined by a terephthalate ligand acting as a μ_2 donor: only one oxygen atom of each carboxylate group links a copper ion of each dinuclear node. Thus, the described features lead to different environments for the copper atoms of the same dinuclear unit. In this way, Cu11 is N_2O_3 pentacoordinate, with a τ parameter[12] (0.03) in agreement with a slightly distorted square pyramid geometry. In this pyramid, O103 occupies the apex. Regarding Cu12, this can be considered as tetracoordinate in a square planar environment, although the distance Cu12···O10 (2.55 Å) seems to indicate a second order interaction.

As a result, both copper atoms of the same dinuclear moiety share the N103C120N104 imidazolidine bridge as a basal vertex and O103 as a basal-apical vertex. This double bridge leads to a Cu···Cu separation of 3.2454(3) Å within the $[Cu_2L^1]^+$ unit, whereas the shortest distance between the copper ions of different cations (Cu11···Cu12′) is 10.2545(4) Å. This value is similar to those found in the literature for other copper complexes with terephthalate bridges coordinated in the same mode.[9,13]

3·9H₂O

An ORTEP view of **3** is shown in Figure 2. Experimental details are given in Table 5, and main distances and angles are listed in Table 2.

The unit cell of **3**·9H_2O is composed of neutral molecules of the pentanuclear complex $[(Cu_2L^1)_2Cu(O_2C\text{-}CH_2\text{-}CO_2)_2]$ and water as solvate. The complex can be considered as being assembled from two dinuclear $[Cu_2L^1]^+$ blocks joined through a mononuclear $[Cu(O_2C\text{-}CH_2\text{-}CO_2)_2]^{2-}$ anion.

Table 2. Main bond lengths (Å) and angles (°) for **3**·9H_2O.[a]

Cu11–O101	1.909(5)	Cu10–O10	1.919(5)
Cu11–N101	1.948(6)	Cu12–O102	1.910(5)
Cu11–O103	1.986(5)	Cu12–N102	1.921(7)
Cu11–N103	2.073(6)	Cu12–O103	1.981(5)
Cu11–O11	2.391(5)	Cu12–N104	2.067(7)
Cu10–O12′	1.900(5)	Cu12–O11	2.372(5)
Cu10–O12	1.900(5)	Cu11···Cu12	3.2124(13)
Cu10–O10′	1.919(5)		
N101–Cu11–O103	158.8(2)	N102–Cu12–O103	159.3(3)
O101–Cu11–N103	175.1(2)	O102–Cu12–N104	176.4(2)
O10′–Cu10–O10	180.0(4)	Cu11–O103–Cu12	108.1(2)
O12′–Cu10–O12	180.0(3)	Cu11–O11–Cu12	84.82(18)

[a] Symmetry operation ′ = $-x + 1, -y, -z$.

Compound **3** also shows an inversion centre located on Cu10, which makes both halves crystallographically equivalent.

If we only consider the $[Cu_2L^1]^+$ cations, as occurred in **1**, each ligand compartment forms a N_2O_2 coordinative environment around each copper(II) ion. These two cations are bridged by a $[Cu(O_2C\text{-}CH_2\text{-}CO_2)_2]^{2-}$ anion, where the copper atom Cu10 is coordinated to two malonate ligands acting as bidentate chelates, with only one oxygen atom of each carboxylate group (O10 and O12) linked to Cu10. Hence, the central copper atom is tetracoordinate, with a perfect square plane geometry, and the donor O atoms and the copper(II) ion lie on the same plane. Even, the whole malonate ligands present a marked planarity, because the farther atom to this plane is the methylene C11 atom, at about 0.33 Å. One of the uncoordinated oxygen atoms of each malonate ligand (O11) acts as a μ_2-η^1:η^1 connector between the $[Cu_2L^1]^+$ and $[Cu(O_2C\text{-}CH_2\text{-}CO_2)_2]^{2-}$ frag-

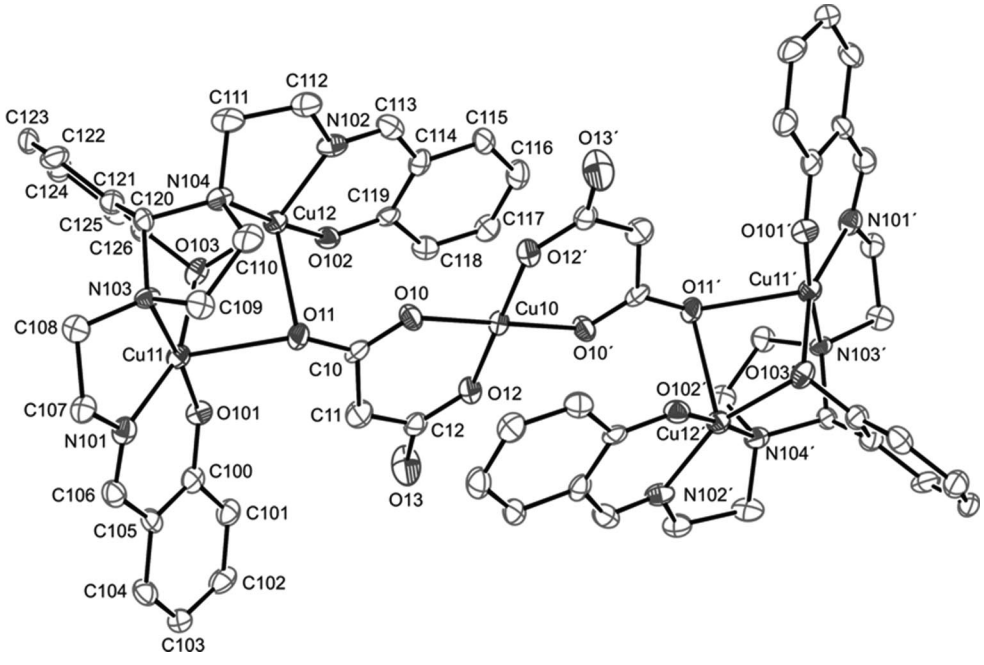

Figure 2. An ORTEP view of the crystal structure of **3**. Hydrogen atoms are omitted for clarity. Ellipsoids are drawn at 40% probability.

ments. Therefore, Cu1*X* (*X* = 1, 2) and Cu10 interact thorough a carboxylate group in a *syn–anti* disposition between Cu12 and Cu10 and in an *anti–anti* disposition between Cu11 and Cu10.

As a result, the four metal centres allocated by the Schiff base ligands are actually N_2O_3 pentacoordinate, with τ values (0.272 for Cu11 and 0.285 for Cu12) that agree with a distorted square pyramidal geometry. These pyramids share O103 as a basal vertex and O11 as the apex. Accordingly, the copper atoms are triple bridged (NCN, O_{phenol}, $O_{carboxylate}$), with a Cu11···Cu12 distance of 3.2124(13) Å. In addition, the distances between the copper ions of each dinuclear unit and that of the mononuclear fragment, bridged by the malonate ligand, reflect the different disposition of the Cu–OCO–Cu fragments. In this way, the distance between the copper atoms connected through the *anti–anti* carboxylate [*d*(Cu11···Cu10) = 6.2814(12) Å] is significantly longer than that between the copper atoms joined through the *syn–anti* one [*d*(Cu12···Cu10) = 4.7861(11) Å], as expected for copper malonate complexes with this coordination mode.[14]

4·5·5H₂O·1.25MeOH

An ORTEP view of **4** is shown in Figure 3. Experimental details are given in Table 5, and main distances and angles are also listed in Table 3.

This complex is a tetranuclear compound as well, which apart from neutral molecules of $[(Cu_2L^2)_2(O_2C\text{-}CH_2\text{-}CO_2)]$ contains methanol and water molecules as solvates in its unit cell. Similarly to that told for **1**, **4** can be also understood as formed from two dinuclear $[Cu_2L^2]^+$ tectons, with the Schiff base ligand again supplying a N_2O_2 environment to each copper atom, but which in this case are joined through a doubly deprotonated malonate ligand. Accordingly, in spite of the close similarities, some remarkable differences are noteworthy and will be explained below.

Table 3. Main bond lengths (Å) and angles (°) for **4**·5.5H_2O·1.25MeOH.

Cu11–O101	1.903(7)	Cu21–O201	1.932(6)
Cu11–N101	1.922(7)	Cu21–N201	1.948(7)
Cu11–O103	1.964(6)	Cu21–O203	1.975(5)
Cu11–N103	2.112(7)	Cu21–N203	2.110(8)
Cu11–O11	2.112(6)	Cu21–O21	2.136(6)
Cu12–O102	1.911(6)	Cu22–O202	1.936(6)
Cu12–O103	1.963(6)	Cu22–N202	1.965(7)
Cu12–N102	1.967(7)	Cu22–O203	1.988(5)
Cu12–N104	2.088(7)	Cu22–N204	2.075(7)
Cu12–O12	2.154(6)	Cu22–O22	2.162(6)
Cu11···Cu12	3.2944(15)	Cu21···Cu22	3.3356(15)
O101–Cu11–N103	172.7(3)	O201–Cu21–N203	166.8(3)
N101–Cu11–O103	150.0(3)	N201–Cu21–O203	157.2(3)
O102–Cu12–N104	166.2(3)	O202–Cu22–N204	170.1(2)
O103–Cu12–N102	155.0(3)	N202–Cu22–O203	155.3(2)
Cu11–O103–Cu12	114.1(3)	Cu21–O203–Cu22	114.7(3)

Thus, in this case the four copper(II) ions are connected through a μ_4:η^1:η^1:η^1:η^1-*O,O′,O″,O‴* bridge, which completes the coordination spheres of the metal ions. Therefore, the four metal centres are pentacoordinate, with distorted

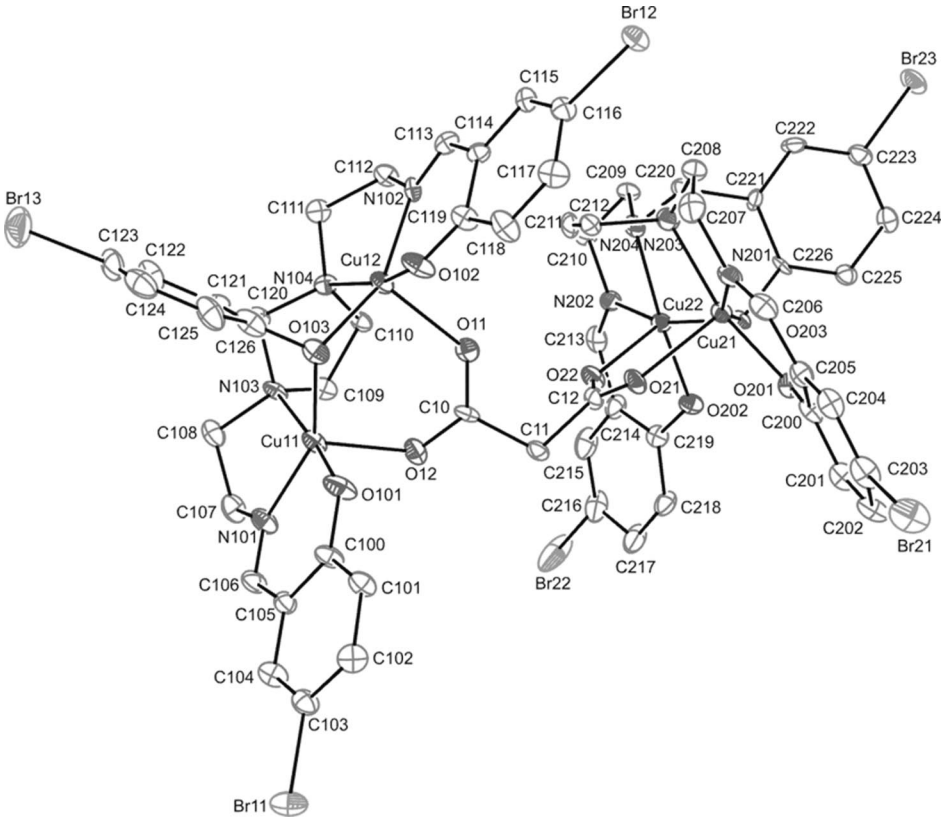

Figure 3. An ORTEP view of the crystal structure of **4**. Hydrogen atoms are omitted for clarity. Ellipsoids are drawn at 40% probability.

square pyramidal geometries (τ values of 0.378 for Cu11, 0.187 for Cu12, 0.160 for Cu21 and 0.248 for Cu22). In these pyramids, the oxygen atoms of the malonate ligand occupy the apical sites. Besides, the pyramids of each dinuclear moiety share the phenol oxygen atom of the central arm (O*X*03, with X = 1, 2) as a basal vertex. This disposition leads to distances between the triply bridged metal atoms of ca. 3.3 Å.

In this complex, in contrast with **3**, the malonate dianion is not planar, as its two carboxylate groups form an angle of about 78.1°, whereas they are only slightly twisted in **3** (ca. 7.9°). This can be attributed to the flexibility provided by the central methylene group of the malonate ligand, which allows a different spatial arrangement of the global complex, if compared with **1** and **3**. In fact, the connectors of these two latter complexes lead to a similar disposition, with an inversion centre situated on the middle of the central connector, so their $[Cu(L^1)]^+$ units are logically inverted. In contrast, the shortest distances between copper(II) ions of different dinuclear units in **4** are longer and are significantly different [Cu12···Cu22 distance of 6.7104(18) Å and Cu11···Cu21 distance of 8.194(2) Å].

Magnetic Studies

The magnetic properties of **1**·7H_2O, **3**·9H_2O and **4**·5.5H_2O were investigated in the 2–300 K temperature range.

The plot of $\chi_M T$ vs. T for **1**·7H_2O is shown in Figure 4, where it can be seen that the $\chi_M T$ product is nearly constant in the range 300–100 K, and it then increases until 8 K and finally quickly decreases at low temperature. Accordingly, the shape of the curve agrees with a predominant intramolecular ferromagnetic coupling. Besides, the $M/N\beta$ vs. H curve at 2 K (Figure 5) tends to 4 (4.05) at 50000 G, which seem to suggest an S = 2 ground state, although a mixture of states cannot be ruled out.

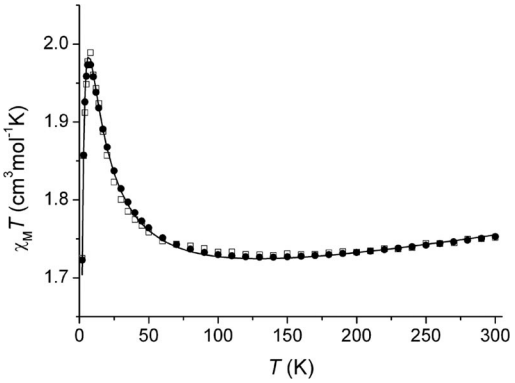

Figure 4. Plot of $\chi_M T$ vs. T for **1**·7H_2O. Experimental results (□), best fit without intermolecular interactions (—), best fit including the intermolecular interactions term (●).

The structural analysis of **1**·7H_2O reveals two different superexchange pathways (Scheme 2). Thus, in view of the $\chi_M T$ vs. T graph, the diminishment of the $\chi_M T$ values at low temperature could be associated with a small intramolecular antiferromagnetic contribution, the presence of antiferromagnetic intermolecular interactions or the effect of the zero-field splitting (ZFS) of the ground state.

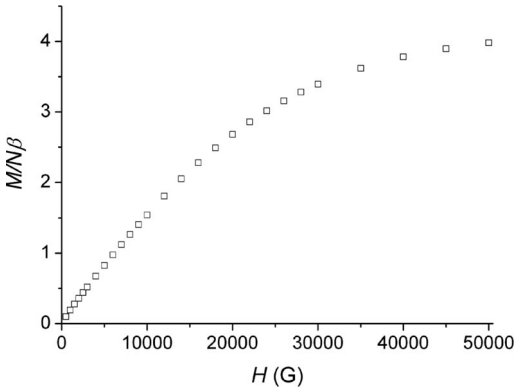

Figure 5. Plot of $M/N\beta$ vs. H at 2 K for **1**·7H_2O.

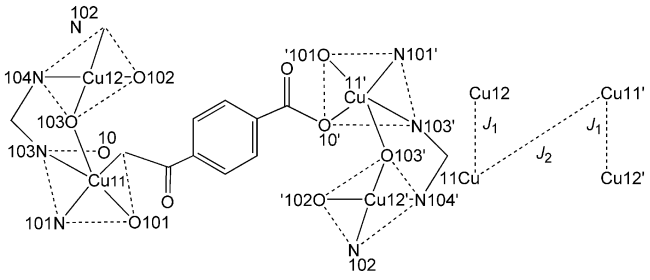

Scheme 2.

Accordingly, the susceptibility curve was treated with the MAGPACK program,[15] where the exchange spin Hamiltonian is expressed as $H = -2\Sigma J_{ij} S_i S_j$. In a first approach, a simple model with the lowest number of parameters was chosen. Thus, a 2J model (Scheme 2), which additionally incorporates the *TIP* parameter, was used to reproduce the experimental data. The best fit with this model renders an S = 0 calculated ground state and the following parameters: $2J_1$ = 10.7 cm^{-1}, $2J_2$ = –1.7 cm^{-1}, g = 2.09 and *TIP* = 3.20×10^{-4} cm^{3}mol^{-1} ($R = 1.88 \times 10^{-5}$). In a second approach, the antiferromagnetic intermolecular interactions or the effect of the zero-field splitting of the ground state was taken into account. As the MAGPACK program only considers D_{local} and not D_{total}, the chosen model is now a 2J model that furthermore includes the intermolecular interactions and *TIP* variables. The best fit with this model gives the parameters: $2J_1$ = 10.9 cm^{-1}, $2J_2$ = 0.8 cm^{-1}, g = 2.09, J' = –0.37 cm^{-1} and *TIP* = 2.95×10^{-4} cm^{3}mol^{-1} ($R = 1.18 \times 10^{-5}$), with an S = 2 calculated ground state. Both fits (Figure 4) produce nearly superimposable graphs and give rise to very similar values of J_1; the J_2 values are positive or negative but small in any case.

The reliability of the obtained parameters was checked by comparison with the literature. Thus, J_1 reflects the magnetic interaction between two Cu^{II} ions mediated by a NCN and a O_{phenol} bridge (Scheme 2). The NCN link is in the basal plane of both square pyramids, whereas the oxygen bridge is basal-apical. Therefore, the magnetic exchange

through this latter pathway must be small. Accordingly, the main magnetic interaction is mediated by an imidazolidine NCN link that, as DFT calculations demonstrated,[7a] should transmit a net ferromagnetic coupling, as it is. Besides, the magnitude of J_1 is in the order of the expected one for this situation.[7a,16]

J_2 represents the magnetic coupling between Cu11 and Cu11′, mediated by the terephthalate ligand, coordinated as shown in Scheme 2. This coordination mode leads to a distance of ca. 10.25 Å between both copper atoms, and therefore, the magnetic exchange between them is expected to be weak. The small value obtained for J_2 is in agreement with the previous discussion and within the values reported in the literature for this type of situation.[9]

The $\chi_M T$ vs. T graph for pentanuclear complex **3**·9H_2O is shown in Figure 6. Once again, the $\chi_M T$ product remains almost constant between 300 and 150 K and then increases with decreasing temperature to reach a maximum. After that, it slightly decreases on cooling. Thus, once more, this behaviour suggests a net intramolecular ferromagnetic coupling. In addition, the magnetic measurements at 2 K shows that the $M/N\beta$ vs. H curve (Figure 7) tends to 4 at 50000 G, suggesting a nonisolated ground state but a mixing of an S = 1.5 and S = 2.5 states.

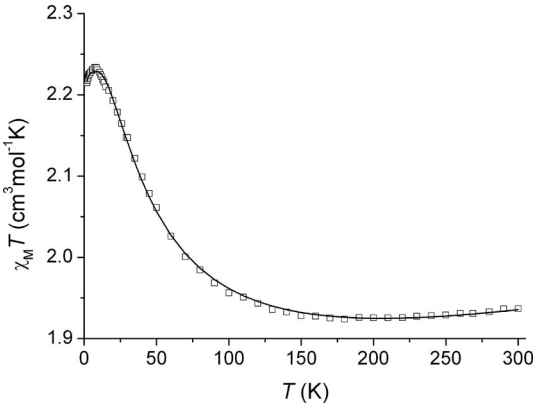

Figure 6. Plot of $\chi_M T$ vs. T for **3**·9H_2O. Scattered points: experimental results; solid line: best fit.

The possible superexchange pathways for **3** are shown in Scheme 3. Accordingly, the $\chi_M T$ vs. T curve was treated with the MAGPACK program, with a 3J model, including

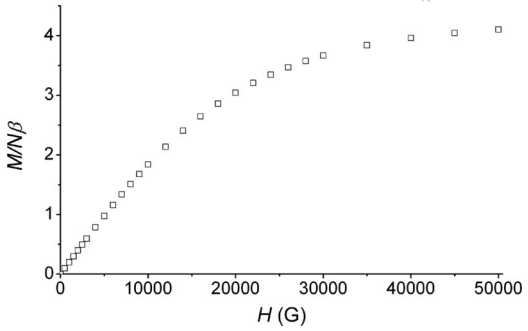

Figure 7. Plot of $M/N\beta$ vs. H at 2 K for **3**·9H_2O.

the intermolecular interaction parameter and *TIP*. The best fit gives the values: $2J_1$ = 37.3 cm^{-1}, $2J_2$ = 0.3 cm^{-1}, $2J_3$ = –0.4 cm^{-1}, g = 1.94, J' = 0 cm^{-1} and *TIP* = 3.87×10^{-4} $cm^3 mol^{-1}$ ($R = 2.06 \times 10^{-6}$). These values render an S = 2.5 ground state, and they seem to justify the mixing of the S = 2.5 and S = 1.5 states (ΔE = 0.17 cm^{-1}). Besides, they appear to be consistent with those expected. Thus, J_1 represents the interaction between CuX1···CuX2 (X = 1, 2) mediated by the NCN and O103 bridges, both of them situated in the basal plane of the square pyramids. In addition, both pyramids share an oxygen carboxylate atom (O11) as the apex, but this bridge should slightly contribute to the magnetic exchange. Therefore, this magnetic superexchange pathway is very similar to one of the magnetic pathways for $[(Cu_2L^1)_2(CO_3)]$·8H_2O, where DFT calculations estimate a coupling constant close to 30 cm^{-1}.[7a]

J_2 and J_3 represent the magnetic exchange within the terminal and central copper atoms, mediated by the carboxylate groups of the malonate ligand, in a *syn–anti* (J_2) or *anti–anti* (J_3) mode. Moreover, it is noticeable that one of the oxygen atoms of the malonate ligand is always at the apex of the pyramid (O11 or O11′) and the other one is at the base of the square plane (O10 or O10′). Therefore, these are basal-apical interactions and they should be small. In addition, it is well known that carboxylate bridges coordinated in a *syn–anti* mode transmit a ferromagnetic coupling and in an *anti–anti* mode an antiferromagnetic interaction.[17] Accordingly, J_2 should be small and positive and J_3 small and negative, as they are.

The $\chi_M T$ vs. T graph for **4**·5.5H_2O (Figure 8) suggests, once more, an intramolecular ferromagnetic coupling be-

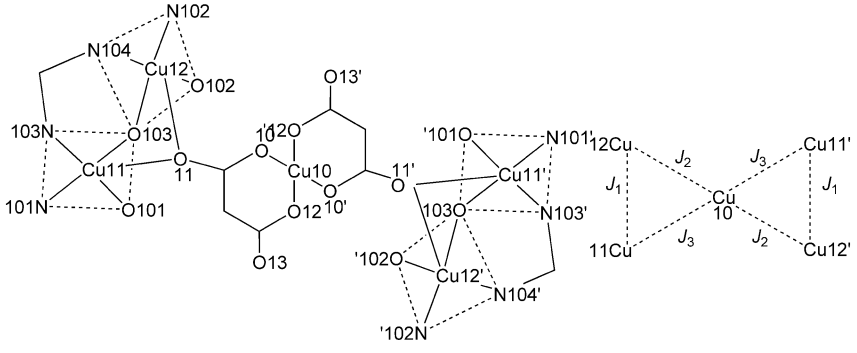

Scheme 3.

tween the copper ions. Besides, the $M/N\beta$ vs. H curve at 2 K (Figure S1, Supporting Information) tends to 4 at 50000 G, which, once more, seems to indicate an $S = 2$ ground state, in spite of the fact that a mixture of states cannot be completely excluded.

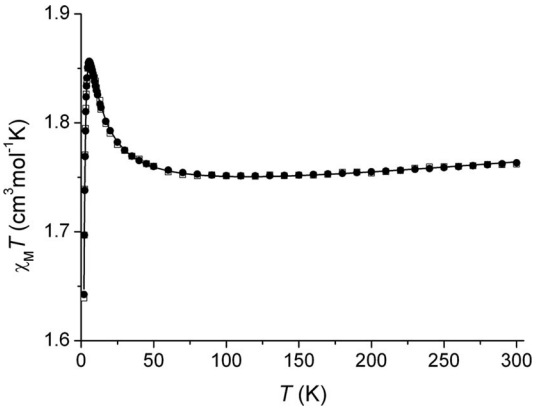

Figure 8. Plot of $\chi_M T$ vs. T for **4**·5.5H_2O. Experimental results (□), best fit without intermolecular interactions (—), best fit including the intermolecular interactions term (●).

Compound **4**·5.5H_2O shows three different magnetic exchange pathways (Scheme 4). Hence, the susceptibility data were treated with the MAGPACK program using a 3J model. It must be noted that, in a first attempt, we tried to fit the data with the lowest number of parameters, that is, excluding intermolecular interactions and/or ZFS. This fit, which renders an $S = 0$ ground state, give the following magnetic parameters: $2J_1 = 3.5\ cm^{-1}$, $2J_2 = -0.3\ cm^{-1}$, $2J_3 = -0.7\ cm^{-1}$, $g = 2.14$ and $TIP = 1.07 \times 10^{-4}\ cm^3\,mol^{-1}$ ($R = 9.31 \times 10^{-7}$). A new fit was also performed with the 3J model including the intermolecular interactions. This gives as the best-fitting parameters $2J_1 = 3.7\ cm^{-1}$, $2J_2 = 1.1\ cm^{-1}$, $2J_3 = 0.2\ cm^{-1}$, $g = 2.14$, $J' = -0.60\ cm^{-1}$ and $TIP = 1.19 \times 10^{-4}\ cm^3\,mol^{-1}$ ($R = 3.58 \times 10^{-7}$), with an $S = 2$ calculated ground state.

Analysis of the data shows that the values of the magnetic parameters are in the range of those expected. Thus, J_1 represents the magnetic interaction between two copper(II) ions mediated by a NCN, a O_{phenol} bridge and a carboxylate link in a *syn–syn* mode, this latter occupying the apexes of the square pyramids. Therefore, the carboxylate bridge should poorly contribute to the magnetic exchange. Accordingly, this superexchange pathway is very similar to that reported for **3**·9H_2O. In this kind of copper compound, where the interaction between the copper atoms is mainly transmitted through a $NCN_{imizadolidine}$ and an O bridge, the magnetic interaction depends not only on the Cu–O_{basal}–Cu angle but on the angle (θ) between the square planes of the pyramids.[6c] When both factors are analysed and compared with those of a series of Cu^{II} complexes derived from H_3L^1 or H_3L^2 (Table 4, Scheme 5), it can be seen that the J_1 value is in agreement with the large Cu–O_{basal}–Cu angle and the acute θ angle.

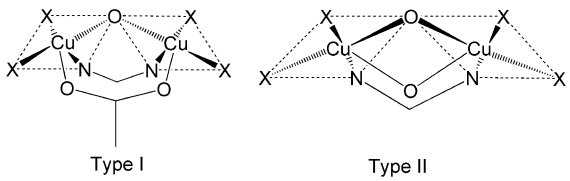

Scheme 5.

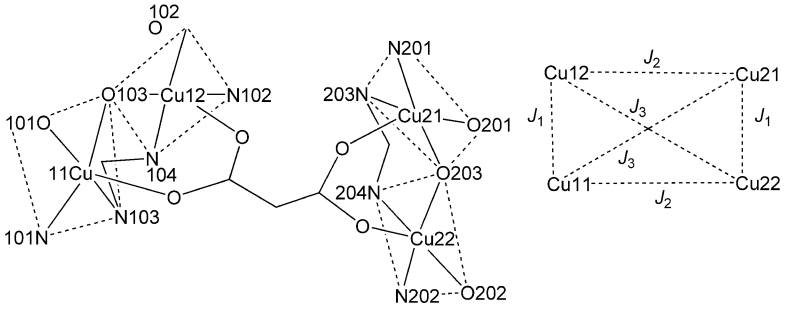

Scheme 4.

Table 4. Some magnetostructural parameters for copper complexes with basal $NCN_{imidazolidine}$ and O bridges.

	a(Cu–O_R–Cu) (°)	θ[a] (°)	μ-OR	$2J$[b] (cm^{-1})	Geometry type[c]	Ref.[d]
[$(Cu_2L^2)_2(O_2C\text{-}CH_2\text{-}CO_2)$] (**4**)	114.4	31.3	PhO	3.3	I	*
[$Cu_2L^2(OAc)$]	113.7	33.0	PhO	11.5	I	[6c]
[$(Cu_2L^1)_2(CO_3)$]	112.0	37.0	PhO	≈30	I	[7a]
[$(Cu_2L^1)_2Cu(O_2C\text{-}CH_2\text{-}CO_2)_2$] (**3**)	108.1	45.3	PhO	37.3	II	*
[$Cu_2L^1(OAc)$]	102.5	46.0	PhO	49.2	II	[6a]
[$Cu_2L^1(CH_3O)$]	104.0	117.0	MeO	82.1	II	[6b]
[$Cu_2L^2(CH_3O)$]	106.0	119.6	MeO	99.9	II	[6c]

[a] Angle between basal planes of the square pyramids. [b] J values referred to Hamiltonian $H = -2JS_iS_j$. [c] Geometry type in Scheme 5. [d] * = this work.

J_2 and J_3 represent the magnetic interaction within the copper atoms through the malonate ligand and, once more, the oxygen atoms of this malonate ligand occupy apical sites. Therefore, the values of J_2 and J_3 should be small, as they are. However, they could be interchangeable, as they could not be compared with literature values. As far as we know, this is the first magnetostructural characterised copper(II) complex with a malonate ligand coordinated in a μ_4:η^1:η^1:η^1:η^1-*O,O′,O′′,O′′′* mode occupying apical sites and the magnetic analysis indicates that it transmit a weak coupling.

Conclusions

Three new Cu_4 (**1**·7H_2O, **2**·2H_2O and **4**·5.5H_2O) clusters and one Cu_5 (**3**·9H_2O) cluster have been prepared from ligand-exchange reactions. The crystal structure of three of them show that all the compounds can be considered as constructed from dinuclear $[Cu_2L^x]^+$ (x = 1, 2) blocks and different carboxylate connectors. Therefore, this work clearly shows that the tested synthetic method allows complexes of higher nuclearity to be constructed from $[Cu_2L^x]^+$ (x = 1, 2) nodes.

Magnetic studies for **1**·7H_2O, **3**·9H_2O and **4**·5.5H_2O show that all the complexes are predominantly ferromagnetic in nature; the magnetic coupling mediated by the dicarboxylate ligands is weak. In addition, it is noteworthy that this paper describes the first magnetostructural characterisation of a copper(II) complex with a malonate ligand coordinated in a μ_4:η^1:η^1:η^1:η^1-*O,O′,O′′,O′′′* mode placed at apical sites.

Experimental Section

General Considerations: Elemental analyses of C, H and N were performed with a Carlo Erba EA 1108 analyzer. Infrared spectra were recorded as KBr pellets with an FTIR Bruker IFS-66v spectrophotometer in the range 4000–400 cm^{-1}. Electrospray mass spectra of the metal complexes were obtained with a Hewlett–Packard LC–MS spectrometer, in methanol as solvent.

Syntheses: All solvents, malonic and terephthalic acid are commercially available and were used without further purification. $[(Cu_2L^1)_2(CO_3)]$·8H_2O and $[Cu_2L^2(OH)]$·1.125H_2O were obtained as previously reported,[6c,7a] and satisfactorily characterised.

1·7H_2O: To a methanol (40 mL) solution of $[(Cu_2L^1)_2(CO_3)]$·8H_2O (0.19 g, 0.14 mmol) was added terephthalic acid (0.023 g, 0.14 mmol). The mixture was heated to reflux with stirring for 3 h, and the green solid that precipitated was filtered off and dried in air. Yield: 0.15 g (73.7%). M.p. >300 °C. $C_{62}H_{76}Cu_4N_8O_{17}$ (1454.13): calcd. C 51.16, H 4.95, N 7.70; found C 50.69, H 4.20, N 7.58. MS (ESI+): m/z = 582.1 $[Cu_2L^1]^+$. IR (KBr): $\tilde{\nu}$ = 1633 (C=N), 3441 (OH) cm^{-1}. Recrystallisation of a microcrystalline sample of **1**·7H_2O in MeOH/EtOH allowed green single crystals of **1**·2EtOH·2H_2O, suitable for X-ray diffraction studies, to be isolated.

2·2H_2O: To a methanol (40 mL) solution of $[Cu_2L^2(OH)]$·1.125H_2O (0.14 g, 0.16 mmol) was added terephthalic acid (0.014 g, 0.08 mmol). The mixture was heated to reflux with stirring for 3 h, and the dark green solid that precipitated was filtered off and dried in air. Yield: 0.092 g (62.6%). M.p >300 °C. $C_{62}H_{56}Br_6Cu_4N_8O_{12}$ (1837.6): calcd. C 40.49, H 3.05, N 6.09; found C 40.04, H 2.99, N 5.91. MS (ESI+): m/z = 818.5 $[Cu_2L^2]^+$. IR (KBr): $\tilde{\nu}$ = 1633 (C=N), 3441 (OH) cm^{-1}.

3·9H_2O: To a MeOH/MeCN (20:20 mL) solution of $[(Cu_2L^1)_2(CO_3)]$·8H_2O (0.1 g, 0.07 mmol) was added malonic acid (0.007 g, 0.07 mmol). The mixture was heated to reflux with stirring for 3 h, and the green precipitated solid was filtered off and dried in air. Yield: 0.038 g (68.1%). M.p >300 °C. $C_{60}H_{76}Cu_5N_8O_{23}$ (1593.75): calcd. C 45.18, H 4.77, N 7.03; found C 45.86, H 4.48, N 7.01. MS (ESI+): m/z = 582.3 $[Cu_2L^1]^+$. IR (KBr): $\tilde{\nu}$ = 1636 (C=N), 3429 (OH) cm^{-1}. Recrystallisation of the microcrystalline solid in MeOH yielded **3**·9H_2O as green single crystals suitable for X-ray diffraction studies.

4·5.5H_2O: To a MeOH/MeCN (20:20 mL) solution of $[Cu_2L^2(OH)]$·1.125H_2O (0.14 g, 0.16 mmol) was added malonic acid (0.0085 g, 0.08 mmol). The mixture was heated to reflux with stirring for 3 h, and the green precipitated solid was filtered off and dried in air.

Table 5. Crystal data and structure refinement for **1**·2EtOH·2H_2O, **3**·9H_2O and **4**·5.5H_2O·1.25MeOH.

	1·2EtOH·2H_2O	**3**·9H_2O	**4**·5.5H_2O·1.25MeOH
Empirical formula	$C_{66}H_{74}Cu_4N_8O_{14}$	$C_{60}H_{61}Cu_5N_8O_{23}$	$C_{58.25}H_{66}Br_6Cu_4N_8O_{16.75}$
Formula weight	1457.49	1579.87	1879.81
Temperature (K)	100(2)	100(2)	100(2)
Wavelength (Å)	0.71073	0.71073	0.71073
Crystal system	monoclinic	monoclinic	orthorhombic
Space group	$P2_1/c$	$P2_1/c$	$P2_12_12_1$
a (Å)	20.0314(7)	9.6724(9)	15.951(3)
b (Å)	9.6076(3)	18.2891(16)	16.340(3)
c (Å)	16.1353(5)	18.9534(17)	27.028(4)
α (°)	95.650(2)	101.133(2)	90
β (°)	20.0314(7)	9.6724(9)	15.951(3)
γ (°)	9.6076(3)	18.2891(16)	16.340(3)
Z	2	2	4
Absorption coefficient (mm^{-1})	1.433	1.674	4.664
Reflections collected	71533	28190	63580
Independent reflections	11875 [R_{int} = 0.0264]	6238 [R_{int} = 0.0599]	15597 [R_{int} = 0.0548]
Data/restraints/parameters	11875/0/418	6238/0/431	15597/0/833
R_1, wR_2 [$I>2\sigma(I)$]	0.0354, 0.0952	0.0772, 0.2018	0.0611, 0.1578
R_1, wR_2 (all data)	0.0470, 0.0994	0.1339, 0.2343	0.0734, 0.1639

Yield: 0.079 g (53.7%). M.p. >300 °C. $C_{57}H_{61}Br_6Cu_4N_8O_{15.5}$ (1838.4): calcd. C 37.2, H 3.32, N 6.09; found C 37.6, H 3.17, N 6.05. MS (ESI+): m/z = 818.3 $[Cu_2L^2]^+$. IR (KBr): $\tilde{\nu}$ = 1635 (C=N), 3436 (OH) cm^{-1}. Green single crystals of **4**·5.5H_2O·1.25MeOH, suitable for X-ray diffraction studies, were obtained by recrystallisation of **4**·5.5H_2O in MeOH.

Crystallographic Measurements: Selected crystal data and some details of refinements are given in Table 5. Crystals of **1**·2EtOH·2H_2O, **3**·9H_2O and **4**·5.5H_2O·1.25MeOH, suitable for single-crystal X-ray studies, were obtained as detailed above. Data were collected at 100 K with a Bruker X8 KappaAPEXII (**1**·2EtOH·2H_2O) or a Smart-CCD-1000 (**3**·9H_2O and **4**·5.5H_2O·1.25MeOH) diffractometer, employing graphite-monochromated Mo-K_α (λ = 0.71073 Å) radiation in all cases. The data reduction procedure involved corrections for polarisation and Lorentz effect, whereas a multiscan absorption correction was applied by using SADABS.[18] The structures were solved by direct methods employing SIR-2004,[19] and refined by full-matrix least-squares on F^2 using the SHELX-97[20] program package. Non-hydrogen atoms were anisotropically refined, excluding some corresponding to disordered solvated molecules. Hydrogen atoms were mostly included at geometrically calculated positions with thermal parameters derived from the parent atoms. Partial occupancies of solvate molecules were individually refined and then rounded to simplify the formulae. It should be noted that **3**·9H_2O shows a marked disorder of its solvates. In this way, most of the water molecules had to be modelled with very low occupation sites, and their H atoms could not be mostly located.

CCDC-762477 (for **1**·2EtOH·2H_2O), -762478 (for **3**·9H_2O) and -762479 (for **4**·5.5H_2O·1.25MeOH) contain the supplementary crystallographic data for this paper. These data can be obtained free of charge from The Cambridge Crystallographic Data Centre via www.ccdc.cam.ac.uk/data_request/cif.

Magnetic Measurements: Magnetic susceptibility measurements for powder crystalline samples of **1**·7H_2O, **3**·9H_2O and **4**·5.5H_2O were carried out at the Unitat de Mesures Magnètiques of the Universitat de Barcelona with a Quantum Design SQUID MPMS-XL susceptometer. The magnetic susceptibility data were recorded in the 2–300 K temperature range under magnetic fields of 300 G (2–30 K) and 5000 G (30–300 K). Diamagnetic corrections were estimated from Pascal's Tables The agreement factor is based on the function $R = \Sigma(\chi_M T_{exp} - \chi_M T_{cal})^2/\Sigma(\chi_M T_{exp})^2$. Magnetic fields ranging from 0 to 50000 G were used for magnetisation measurements at 2 K.

Supporting Information (see footnote on the first page of this article): Plot of $M/N\beta$ vs. H at 2 K for **4**·5.5H_2O.

Acknowledgments

The research reported here was supported by Xunta de Galicia (PGIDTIT06PXIB209043PR).

[1] O. Kahn, *Molecular Magnetism*, VCH, New York, **1993**.
[2] J. Ribas, A. Escuer, M. Monfort, R. Vicente, R. Cortés, L. Lezama, T. Rojo, *Coord. Chem. Rev.* **1999**, *195*, 1027–1068.
[3] G. Christou, D. Gatteschi, D. N. Hendrickson, R. Sessoli, *MRS Bull.* **2000**, *25*, 66–71.
[4] R. E. P. Winpenny in *Comprehensive Coordination Chemistry II*, **2004**, vol. 7, pp. 125–175.
[5] a) R. W. Gable, B. F. Hoskins, R. Robson, *J. Chem. Soc., Chem. Commun.* **1990**, 1677–1678; b) B. F. Hoskins, R. Robson, *J. Am. Chem. Soc.* **1990**, *112*, 1546–1554.
[6] a) M. Fondo, A. M. García-Deibe, J. Sanmartín, M. R. Bermejo, L. Lezama, T. Rojo, *Eur. J. Inorg. Chem.* **2003**, 3703–3706; b) M. Fondo, A. M. García-Deibe, M. Corbella, J. Ribas, A. L. Llamas-Saiz, M. R. Bermejo, J. Sanmartín, *Dalton Trans.* **2004**, 3503–3507; c) M. Fondo, N. Ocampo, A. M. García-Deibe, M. Corbella, M. R. Bermejo, J. Sanmartín, *Dalton Trans.* **2005**, 3785–3794; d) M. Fondo, A. M. García-Deibe, N. Ocampo, J. Sanmartín, M. R. Bermejo, A. L. Llamas-Saiz, *Dalton Trans.* **2006**, 4260–4270.
[7] a) M. Fondo, A. M. García-Deibe, M. Corbella, E. Ruiz, J. Tercero, J. Sanmartín, M. R. Bermejo, *Inorg. Chem.* **2005**, *44*, 5011–5020; b) M. Fondo, N. Ocampo, A. M. García-Deibe, E. Ruiz, J. Tercero, J. Sanmartín, *Inorg. Chem.* **2009**, *48*, 9861–9873.
[8] F. S. Delgado, J. Sanchiz, C. Pérez-Ruíz, F. LLoret, M. Julve, *Inorg. Chem.* **2003**, *42*, 5938–5948 and references cited therein.
[9] S. S. Massoud, F. A. Mautner, R. Vicente, H. N. Sweeney, *Inorg. Chim. Acta* **2006**, *359*, 1489–1500 and references cited therein.
[10] R. Baldomá, M. Monfort, J. Ribas, X. Solans, M. A. Maestro, *Inorg. Chem.* **2006**, *45*, 8144–8155 and references cited therein.
[11] D. Martínez, M. Motevalli, M. Watkinson, *Dalton Trans.* **2010**, *39*, 446–455.
[12] A. W. Addison, T. N. Rao, J. Reedijk, J. Van Rijn, C. G. Verschoor, *J. Chem. Soc., Dalton Trans.* **1984**, 1349–1356.
[13] A. Company, L. Gómez, J. P. López Valbuena, R. Mas-Ballesté, J. Benet-Buchholz, A. Llobet, M. Costas, *Inorg. Chem.* **2006**, *45*, 2501–2508.
[14] a) C. Ruiz-Pérez, J. Sanchiz, M. Hernández Molina, F. Lloret, M. Julve, *Inorg. Chem.* **2000**, *39*, 1363–1370; b) J. Sanchiz, Y. Rodríguez-Martín, C. Ruiz-Pérez, A. Mederos, F. Lloret, M. Julve, *New J. Chem.* **2002**, *26*, 1624–1628.
[15] a) J. J. Borrás-Almenar, J. M. Clemente, E. Coronado, B. S. Tsukerblat, *Inorg. Chem.* **1999**, *38*, 6081–6088; b) J. J. Borrás-Almenar, J. M. Clemente, E. Coronado, B. S. Tsukerblat, *J. Comput. Chem.* **2001**, *22*, 985–991.
[16] P. K. Nanda, G. Aromí, D. Ray, *Inorg. Chem.* **2006**, *45*, 3143–3145.
[17] A. Rodríguez-Fortea, P. Alemany, S. Álvarez, E. Ruiz, *Chem. Eur. J.* **2001**, *7*, 627–637.
[18] a) *SADABS*, Area-Detector Absorption Correction, Siemens Industrial Automation, Inc., Madison, WI, **1996**; b) R. H. Blessing, *Acta Crystallogr., Sect. A* **1995**, *51*, 33–38.
[19] SIR2004. M. C. Burla, R. Caliandro, M. Camalli, B. Carrozzini, G. L. Cascarano, L. De Caro, C. Giacovazzo, G. Polidori, R. Spagna, *J. Appl. Crystallogr.* **2005**, *38*, 381–388.
[20] *SHELX97 Programs for Crystal Structure Analysis*, G. M. Sheldrick, *Acta Crystallogr., Sect. A* **2008**, *64*, 112–122.

Received: January 21, 2010
Published Online: April 26, 2010

